Tuning Particle Biodegradation through Polymer-Peptide Blend Composition

*Sylvia T. Gunawan,[†] Kristian Kempe,[†,+] Georgina K. Such,[†,‡] Jiwei Cui,[†] Kang Liang,[†,#] Joseph J. Richardson,[†] Angus P. R. Johnston,[†,§] and Frank Caruso[†,]**

[†]ARC Centre of Excellence in Convergent Bio-Nano Science and Technology, and the Department of Chemical and Biomolecular Engineering, The University of Melbourne, Parkville, Victoria 3010, Australia

KEYWORDS: enzymes, cellular degradation, bioresponsive, drug delivery, mesoporous silica

ABSTRACT

We report the preparation of polymer-peptide blend replica particles via the mesoporous silica (MS) templated assembly of poly(ethylene glycol)-*block*-poly(2-diisopropylaminoethyl methacrylate-*co*-2-(2-(2-(prop-2-ynyloxy)ethoxy)ethoxy)ethyl methacrylate) (PEG_{45}-*b*-P(DPA_{55}-*co*-$PgTEGMA_4$)) and poly(L-histidine) (PHis). PEG_{45}-*b*-P(DPA_{55}-*co*-$PgTEGMA_4$) was synthesized by atom transfer radical polymerization (ATRP), and was co-infiltrated with PHis into poly(methacrylic acid) (PMA)-coated MS particles assembled from different peptide-to-polymer ratios (1:1, 1:5, 1:10, or 1:15). Subsequent removal of the sacrificial templates and PMA resulted in monodisperse, colloidally stable, non-covalently cross-linked polymer-peptide blend replica particles that were stabilized by a combination of hydrophobic interactions between the

PDPA and the PHis, hydrogen bonding between the PEG and PHis backbone, and π-π stacking of the imidazole rings of PHis side chains at physiological pH (pH ~7.4). Synergistic charge-switchable and enzymatic degradation properties of PDPA and PHis make these particles responsive to pH and enzymes. *In vitro* studies, in simulated endosomal conditions and inside cells, demonstrated that particle degradation kinetics could be engineered (from 2 to 8 h inside dendritic cells) based on simple adjustment of the peptide-to-polymer ratio used.

INTRODUCTION

Research into designing therapeutic carriers has progressively advanced, particularly in the development of "smarter", more responsive materials for reducing unwanted side effects and for achieving optimized therapeutic efficacy.[1-5] Different types of polymer carriers, such as polymeric micelles,[6] polymersomes,[7] polymer capsules,[8,9] and polymer replica particles[10] have been developed. The first generation of these materials exploited diffusion-based dissolution kinetics and the semi-permeable nature of the materials themselves as the cargo release mechanisms.[11] However, this approach provided little control over the release kinetics or carrier degradation rate. To improve the functionality of the carriers and consequently the therapeutic outcome, responsive moieties have been incorporated to achieve controlled carrier degradation and/or cargo release.[12-14] Thus, the next generation of carriers comprises multifunctional responsive polymer building blocks and/or inorganic substances that are responsive to stimuli such as electromagnetic radiation, temperature, ultrasound, and near-infrared (NIR)-light.[15-18] Recently, a better understanding of cellular pathways has allowed for the development of advanced systems that respond to the biological milieu inside cells or tissues, such as pH variations, redox potential differences, and the presence of different types of enzymes.[19,20] These

biologically inspired carriers can be engineered to degrade or to release their cargo upon reaching the cellular compartments of interest.

The internalization of particles generally involves an energy dependent endocytotic process where the cell membrane engulfs the particle, forming a vesicle that is transported to specific sub-cellular compartments.[21-23] This pathway generally exposes the particles to a pH gradient where the pH decreases from physiological pH (~7.4) in the extracellular space down to pH 4.5–5.5 in the late endosomes/lysosomes.[24] Various types of enzymes are also present in these compartments.[25] Hence, the use of smart materials that are inherently responsive to the dynamics of cellular microenvironments is of interest for triggered release and/or degradation in particular cellular compartments. Materials with pK_a values within the endosomal and physiological pH window are suitable for exploiting release of materials internalized via endocytotic pathways. One example is poly(2-diisopropylaminoethyl methacrylate) (PDPA) comprising pendant diisopropyl amino groups with a pK_a of ~6.4.[26-31] This polymer has tertiary amine groups that undergo protonation (hydrophilic) or deprotonation (hydrophobic) when the pH is below or above its pK_a, respectively. Poly(L-histidine) (PHis) comprises pendant imidazole groups and is another material with a physiologically relevant pK_a of ~6.1, which also allows for the hydrophilic to hydrophobic switch upon increasing the pH above its pK_a.[32] The similarity of these two polymers (in terms of their pK_a) allows for PDPA to be regarded as a synthetic analog to PHis. Further, it provides an opportunity to create smart carriers utilizing their innate pH-induced charge-switching properties as the driving force for carrier assembly and disassembly. In addition, the use of a polypeptide as a building block is of interest due to the enzyme (protease)-sensitive nature of the material, allowing for its degradation in biological microenvironments.[33,34]

Recently, we demonstrated a templated assembly technique for replica particle formation using mesoporous silica (MS) particles as sacrificial templates.[35-38] This approach is versatile because it is applicable for various synthetic and biopolymers. The infiltration of preformed polymers[35,36,38] or the polymerization of monomers within MS particles,[37] followed by cross-linking and removal of the MS particle template, results in the formation of replica particles with tunable functionalities and properties. However, a cross-linker is generally essential for the stabilization of the polymer networks and the formation of replica particles. We have also previously reported the synthesis of PDPA-based nanoparticles and polymer capsules with single- or dual-responsiveness towards pH,[39-41] redox potential,[42,43] and/or enzymes.[44] However, again, for the dual-responsive capsules mentioned, the additional functionality has been incorporated through the use of degradable cross-linkers. Herein, we utilize the MS templated assembly method to fabricate polymer-peptide blend replica particles via co-infiltration of two components (i.e., PHis and PEG_{45}-*b*-P(DPA_{55}-*co*-$PgTEGMA_4$)), without the use of cross-linkers or covalent modification of the polymers. The use of a two-component blend of PDPA and its natural analogue PHis allows the engineering of replica particles and the simple tuning of the biodegradation rate.

A PDPA-based block copolymer, poly(ethylene glycol)-*block*-poly(2-diisopropylaminoethyl methacrylate-*co*-2-(2-(2-(prop-2-ynyloxy)ethoxy)-ethoxy)ethyl methacrylate) (PEG_{45}-*b*-P(DPA_{55}-*co*-$PgTEGMA_4$)) was synthesized via atom transfer radical polymerization (ATRP). PEG was incorporated to improve overall stability of the particles and alkyne functionalities were added for the potential use of pre- or post-coupling with therapeutics or targeting moieties. The PEG_{45}-*b*-P(DPA_{55}-*co*-$PgTEGMA_4$) and PHis were co-infiltrated into poly(methacrylic acid) (PMA)-coated MS particle templates at different peptide-to-polymer

ratios. Subsequent sacrificial MS particle templates and PMA removal resulted in monodisperse, colloidally stable polymer-peptide blend replica particles, stabilized by a combination of hydrophobic interactions between the PDPA and the PHis, hydrogen bonding between the PEG and PHis backbone, and π-π stacking of the imidazole rings of PHis side chains at physiological pH. It was demonstrated that exposure to protease and endosomal pH induces particle degradation via the enzymatic hydrolysis of PHis, and the protonation of both PDPA and PHis. The biodegradation kinetics of these particles, from 2 to 8 h *in vitro* inside the cells, can be engineered by simple tuning of the peptide-to-polymer ratio co-infiltrated into the MS particle templates. The design of this particulate system is advantageous due to: (i) the use of a simple, versatile (MS) templated assembly method, (ii) the combination of synthetic (PDPA) and biopolymer (PHis) analogs as building blocks, (iii) the exploitation of the material's innate, charge-switchable properties for carrier assembly and disassembly, without cross-linkers, and (iv) the engineered biodegradation kinetics, *in vitro* in simulated endosomal conditions and inside of cells, by simply tuning the peptide-to-polymer ratio during the assembly step.

EXPERIMENTAL SECTION

Materials. Poly(methacrylic acid) (PMA, 15 kDa) and 2-diisopropylaminoethyl methacrylate (DPA) were purchased from Polysciences (Warrington, PA, USA). Alexa Fluor 488 (AF488) azide (triethylammonium salt), AF488 succinimidyl (NHS) ester (triethylammonium salt), Dulbecco's phosphate buffered saline (DPBS), Recombinant Mouse Granulocyte Macrophage Colony-Stimulating Factor (GM-CSF) recombinant mouse protein, and MEM alpha were purchased from Life Technologies (California, USA). Black Hole Quencher 1 (BHQ1) azide was

purchased from Primetech LLC (Minsk, Belarus). Poly(L-histidine) (PHis, 5–25 kDa), anisole, tetrahydrofuran (THF), tetra-*n*-butyl ammonium fluoride (TBAF) (1.0 M THF solution), N,N,N′,N″,N″-pentamethyldiethylenetriamine (PMDETA), copper(I) chloride (CuCl), acetic acid, protease from *Aspergillus oryzae* (≥ 500 U/g), tetraethyl orthosilicate (TEOS), (3-aminopropyl)-triethoxysilane (APTES), cetyltrimethylammonium bromide (CTAB), poly(acrylic acid) (PAA, 250 kDa, 35%), ammonia solution (28–30%), ethanol, sodium acetate (NaOAc), sodium-L-ascorbate, copper (II) sulphate ($CuSO_4$) anhydrous, hydrofluoric acid (HF), ammonium fluoride (NH_4F), 3-(N-Morpholino)propanesulfonic acid (MOPS), phosphate buffered saline (PBS), sodium biphosphate (Na_2HPO_4), and hydrochloric acid (HCl) were purchased from Sigma Aldrich (Sydney, Australia). Fetal bovine serum (FBS) was purchased from JRH Biosciences (Kansas, USA). NAP-25 columns were obtained from GE Healthcare (Buckinghamshire, UK). 2,3-Bis(2-methoxy-4-nitro-5-sulfo-phenyl)-2*H*-tetrazolium-5-carbox-anilide inner salt (XTT) was purchased from Promega (Madison, USA). High purity and resistivity water (Milli-Q gradient A 10 system, resistivity >18 MΩ·cm, TOC < 4 ppb, Millipore Corporation, Massachusetts, USA) was obtained from an inline Millipore RiOs/Origin water purification system. All materials were used as received unless otherwise stated. PEG_{45}-bromide (PEG-Br)[45] and 2-(2-(2-(3-(trimethylsilyl)prop-2-ynyloxy)ethoxy)ethoxy)-ethyl methacrylate (TMSPgTEGMA)[43] were prepared according to literature procedures.

Methods. Fluorescence and differential interference contrast (DIC) microscopy images of the replica particles were acquired using an inverted Olympus IX71 microscope. The 60× oil objective lenses and a 488 nm excitation filter were used. A black and white camera mounted on the left port of the microscope was used to capture the microscopy images. For the transmission electron microscopy (TEM) analysis, 3 μL of replica particles was allowed to adsorb onto a

carbon-coated Formvar film mounted on 300-mesh copper grids (ProSciTech, Australia). The grids were blotted dry using a filter paper by placing in a droplet of water (pH ~7.4) for 5 s multiple times. After blotting dry, the grids were air dried overnight and then analyzed using TEM (Philips CM120 BioTWIN, operated at 120 kV). The confocal laser scanning microscopy (CLSM) experiment was performed using a Leica TCS SP2 confocal system equipped with an HCX PL APO lbd.BL 63× 1.4NA oil objective. The images were then analyzed using Imaris software (Bitplane AG). The *in vitro* intracellular degradation experiments were performed using a deconvolution microscope (DeltaVision, Applied Precision, 60× 1.42 NA oil objective). The filter set used was FITC to analyze the AF488 fluorescence. The images were then deconvolved and analyzed using Imaris (Bitplane AG) with maximum intensity projection. Size measurements of the polymer-peptide blend replica particles, prepared from different sizes of MS particle templates, were performed using a Zetasizer (Nano ZS, Malvern). Each measurement was performed 15 times. Quantification of the AF488-labeled PHis or AF488-labeled PEG_{45}-*b*-P(DPA_{55}-*co*-$PgTEGMA_4$) adsorbed onto the MS particle templates was performed using a Fluorog-3 Model FL3-22 spectrofluorometer (Jobin Yvon Inc., USA) equipped with a HgXe lamp, with excitation and emission wavelengths of 495 nm and 519 nm, respectively. Flow cytometry experiments were performed using a Partec Cyflow Space (Partec GmbH, Germany) with Partec CyFlowMax software for the data analysis. The thresholds for FSC and SSC were adjusted for optimum signal-to-noise ratio. Sample solutions were inserted and passed through the laser beam at an excitation length of 488 nm for AF488. The emission in FSC, SSC, and FL1 was observed and plotted on 2D histograms. The cytotoxicity studies were analyzed by measuring the sample absorbance at 450 nm using an Infinite M200 microplate reader (Tecan, Switzerland).

Mesoporous Silica Particle Synthesis. Mesoporous silica particles (MS particles, 1.4 μm-diameter) were synthesized according to a modified literature method.[46] Briefly, PAA (1.60 g) was dissolved in Milli-Q water (16.7 mL), into which CTAB (0.37 g) was added upon vigorous stirring at 25 °C until a clear solution was obtained. Ammonia (1.17 mL) was then added to the mixture with vigorous stirring, which resulted in a milky suspension. After further stirring for 20 min, TEOS (1.48 mL) was added and the mixture was allowed to stir for another 15 min. The mixture was then transferred into an autoclave and incubated at 80 °C for 48 h. The as-synthesized particles were washed twice with Milli-Q water and three times with ethanol. Afterwards, the organic templates were removed by calcination at 550 °C for 6 h. The MS particle surface was then functionalized using a layer of primary amine groups via APTES modification. In this process, the MS particles were dispersed in ethanol (20 mg mL^{-1}) via sonication (Bransonic 1510E-DTH ultrasonic cleaner) for 15 min. APTES and ammonia were then added at a volumetric ratio of 18:1:1 [ethanol]:[APTES]:[ammonia]. The mixture was incubated overnight and the excess reactants were removed through multiple centrifugation/redispersion cycles (1500 *g*, 1 min) in ethanol and Milli-Q water.

Synthesis of poly(ethylene glycol)-*block*-poly(2-diisopropylaminoethyl methacrylate-*co*-2-(2-(2-(3-(trimethylsilyl)prop-2-ynyloxy)ethoxy)ethoxy)ethyl methacrylate) (PEG_{45}-*b*-P(DPA_{55}-*co*-$TMSPgTEGMA_4$)). PEG_{45}-*b*-P(DPA_{55}-*co*-$TMSPgTEGMA_4$) was prepared by atom transfer radical polymerization (ATRP). DPA (736 mg; 3.45 mmol), $TMSPgTEGMA_4$ (328.5 mg; 0.28 mmol), and PMDETA (17.5 mg; 0.1 mmol) were dissolved in anisole (1 mL) and degassed for 30 min. In parallel, PEG-Br (92.8 mg; 0.046 mmol) was dissolved in anisole (1 mL), CuCl (5.4 mg; 0.05 mmol) was added and the suspension was degassed for 30 min. The total monomer concentration was adjusted to 1.4 M with a [DPA]:[TMSPgTEGMA]:[PEG-Br]

ratio of 75:6:1. The DPA solution was added to the CuCl suspension and then reacted at 40 °C for 16 h. After cooling to room temperature (23 °C), the polymer solution was passed through a neutral alumina column to remove the copper. Subsequently, it was dialyzed against THF for 3 days. ^{1}H NMR revealed 73% and 66% conversion for DPA and TMSPgTEGMA$_4$, respectively. ^{1}H NMR (400 MHz, $CDCl_3$, δ): 4.2 – 3.75 (COOCH_2), 3.75 – 3.5 (CH_2CH_2O), 3.2 – 2.85 (CH_2N), 2.85 – 2.5 ((CH$_3$)CHN), 2.25 – 0.6 (backbone), 0.17 ((CH_3)$_3$Si) ppm. SEC (DMAc, PS standard): M_n = 13,200 g mol^{-1}, Đ = 1.28.

Synthesis of poly(ethylene glycol)-*block*-poly(2-diisopropylaminoethyl methacrylate-*co*-2-(2-(2-(prop-2-ynyloxy)ethoxy)ethoxy)ethyl methacrylate) (PEG$_{45}$-*b*-P(DPA$_{55}$-*co*-PgTEGMA$_4$)). For the deprotection of the alkyne groups, PEG$_{45}$-*b*-P(DPA$_{55}$-*co*-TMSPgTEGMA$_4$) (250 mg) and acetic acid (20 μL) were dissolved in THF (2.5 mL), cooled to 0 °C and degassed for 10 min. A 1.0 M solution of TBAF (350 μL) was added slowly via a syringe and the solution was stirred for 1 h at 0 °C followed by stirring at room temperature (23 °C) for 3 h. After passing the solution through a neutral alumina column, the polymer was further purified by dialysis against THF for 2 days. THF was evaporated and PEG$_{45}$-*b*-P(DPA$_{55}$-*co*-PgTEGMA$_4$) was obtained as a slightly yellowish gel. ^{1}H NMR analysis confirmed 100% removal of the TMS-protecting group. ^{1}H NMR (400 MHz, $CDCl_3$, δ): 4.2 – 3.75 (COOCH_2), 3.75 – 3.5 (CH_2CH_2O), 3.2 – 2.85 (CH_2N), 2.85 – 2.5 ((CH$_3$)CHN), 2.25 – 0.6 (backbone) ppm. SEC (DMAc, PS standard): M_n = 14,700 g mol^{-1}, Đ = 1.33.

Pre-labeling of Peptide and Polymer. The pre-labeling of PEG$_{45}$-*b*-P(DPA$_{55}$-*co*-PgTEGMA$_4$) was conducted via a copper(I)-catalyzed alkyne-azide cycloaddition (CuAAC) reaction between the alkyne moieties in PEG$_{45}$-*b*-P(DPA$_{55}$-*co*-PgTEGMA$_4$) and an azide-functionalized dye. PEG$_{45}$-*b*-P(DPA$_{55}$-*co*-PgTEGMA$_4$) (20 mg) was dissolved in 4 mL NaOAc (50 mM, pH 4). A

mixture of 20 μL AF488 azide (1 mg mL^{-1} in DMSO), 500 μL sodium ascorbate (4.4 mg mL^{-1}), and 500 μL copper (II) sulphate (1.8 mg mL^{-1}) was added to the polymer solution and incubated overnight. The pre-labeled polymer was then passed through a NAP-25 column to remove the unreacted dyes and then freeze dried. The pre-labeling of PHis was performed through *N*-hydroxysuccinimide (NHS) chemistry between the NH_2 terminus of PHis and a NHS-functionalized dye. PHis (20 mg) was dissolved in Na_2HPO_4 (100 mM, pH 7.4) and the pH was slowly reduced by dropwise addition of HCl until the polypeptide solution was clear. 20 μL of AF488 NHS (1 mg mL^{-1} in DMSO) was added to the solution and it was allowed to react overnight. The pre-labeled polypeptide was passed through a NAP-25 column to remove the unreacted dyes and then freeze dried.

Particle Preparation. APTES-modified MS particles (1 mg) were washed by three centrifugation/redispersion cycles (1500 *g*, 1 min) in sodium acetate buffer (NaOAc, 50 mM, pH 4.5) and then incubated with PMA (0.1 mg mL^{-1} in Milli-Q, pH 4.5) overnight under constant shaking. The excess polymer was removed by three washes (1500 *g*, 1 min) in NaOAc. Subsequently, PHis (1 mg mL^{-1} in NaOAc, pH 4.5) and PEG_{45}-*b*-P(DPA_{55}-*co*-$PgTEGMA_4$) (1 mg mL^{-1} in NaOAc, pH 4.5) were added to the PMA-coated MS particles with a different peptide-to-polymer volumetric ratio (1:1, 1:5, 1:10, or 1:15) and incubated overnight. The polymer-coated MS particles were then washed three times to remove the excess polymers. To form polymer-peptide blend replica particles, the MS particle core was removed by dispersion in a buffered HF solution (2 M HF and 8 M NH_4F), followed by three centrifugation/redispersion cycles in NaOAc (4500 *g*, 5 min). The sacrificial PMA layers were then removed by multiple washing (4500 *g*, 5 min) in MOPS and finally PBS.

Fluorescent Labeling of Particles. The alkyne moieties in the polymer were used for fluorescent post-labeling of the particles. To the polymer-coated MS particles (a starting amount of 1 mg), a mixture of 1 μL AF488 or BHQ1 azide (1 mg mL^{-1} in DMSO), 100 μL sodium ascorbate (4.4 mg mL^{-1}), and 100 μL copper (II) sulphate (1.8 mg mL^{-1}) were added in 299 μL NaOAc for a CuAAC reaction to occur overnight. The unreacted dyes were removed via three centrifugation/redispersion cycles (1500 *g*, 1 min) in sodium acetate buffer prior to the core removal.

Adsorption Quantification. Particles with different peptide-to-polymer ratios were synthesized using the method mentioned above using either AF488-labeled PHis ($PHis_{488}$) or AF488-labeled PEG_{45}-*b*-P(DPA_{55}-*co*-$PgTEGMA_4$) (PEG_{45}-*b*-P(DPA_{55}-*co*-$PgTEGMA_4$)$_{488}$). Subsequent to the polymer-peptide blend adsorption onto the PMA-coated MS particles, the supernatant was collected and measured using a fluorescence spectrophotometer (Jobin Yvon Inc., USA) to determine the amount of non-adsorbed peptide or polymer, separately. Calibration curves (Figure S1) correlating the fluorescence intensity of $PHis_{488}$ or PEG_{45}-*b*-P(DPA_{55}-*co*-$PgTEGMA_4$)$_{488}$ and their corresponding concentrations were developed to quantify the amount of peptide or polymer adsorbed into the PMA-coated MS particles. The experiments were performed in triplicate.

Particle Stability. Fluorescently labeled particles, with different peptide-to-polymer ratio, were washed into PBS and counted by flow cytometry. Samples of at least 1×10^6 particles were incubated in PBS, pH 7.4 at 37 °C under constant shaking (800 rpm). Approximately 5×10^4 particles were evaluated at each run. The particle count was monitored to assess the stability of linker-free particles under physiological conditions based on hydrophobic interactions between the peptide and the polymer. The experiments were performed in triplicate.

***In Vitro* Particle Degradation.** Fluorescently labeled particles were washed into PBS and counted by flow cytometry. Samples containing at least 1×10^6 particles, assembled from different peptide-to-polymer ratio, were incubated with 5 units mL^{-1} protease (PBS, pH 5.5) at 37 °C under constant shaking (800 rpm). Approximately 5×10^4 particles were assessed for each measurement. The particle count was followed at different incubation periods (up to 6 h) to determine the particle degradation based on the hydrophobic to hydrophilic switch of both PHis and PEG_{45}-*b*-P(DPA_{55}-*co*-$PgTEGMA_4$) and the protease hydrolysis of PHis. The experiments were performed in triplicate.

Particle-Cell Association Kinetics. JAWS II cells were cultured in a complete media (80% MEM alpha, 20% FBS, and 2.5 μL GM-CSF) at 37 °C, 5% CO_2. JAWS II cells were then seeded in a 24-well plate at a population of 70 000 cells per well overnight. Fluorescently labeled particles with different peptide-to-polymer ratio were added at a 20:1 particle-to-cell ratio to each well for different incubation times (1, 2, 3, 4, 5, and 6 h). The cells were kept at 37 °C, 5% CO_2 over the course of the experiment. Cell media was then aspirated and 200 μL of 1× trypsin was added to lift the cells. The cells were then transferred to 1 mL of PBS and the fluorescence intensity of the particles was followed using flow cytometry. The experiments were performed in triplicate.

***In Vitro* Intracellular Degradation.** JAWS II cells were seeded in an 8-chambered cover glass (Thermo Scientific, US) (37 °C, 5% CO_2) overnight at a population of 50 000 cells per well. Particles, assembled from different peptide-to-polymer ratios, comprised of $PHis_{488}$ and PEG_{45}-*b*-P(DPA_{55}-*co*-$PgTEGMA_4$)$_{BHQ1}$ blends. The particles were then added at a 20:1 particle-to-cell ratio. After 1 h incubation, the cell media was aspirated to remove the unbound particles and

replaced with a warm media (37 °C). To observe the intracellular degradation, live cell imaging was performed using a DeltaVision (Applied Precision) microscope equipped with a cell incubation chamber (with 5% CO_2 inlet stream and a temperature control at 37 °C). Live cell imaging was manually performed at five random spots for each incubation time and images were taken on a series of z-sections in between the top and bottom of the cells. Images were then deconvolved and analyzed using Imaris (Bitplane) software for the maximum intensity projection.

Cytotoxicity Assay. JAWS II cells were seeded in a 96-well plate overnight at a population of 5000 cells per well. Particles with different peptide-to-polymer ratios were added to the cells at a particle-to-cell ratio of 1:1, 5:1, 10:1, 50:1, and 100:1 in 200 μL complete media. Subsequent to 48 h incubation, the cell media was aspirated and replaced with an XTT assay solution (0.91 mg mL^{-1} XTT, 1.8% v/v DMSO, and 0.14 mg mL^{-1} PMS) for 5 h. The absorbance at 450 nm was measured using an Infinite M200 microplate reader (Tecan, Switzerland) to evaluate the particle cytotoxicity. The experiments were performed in quadruplicate.

RESULTS AND DISCUSSION

Synthesis of PEG_{45}-*b*-($PDPA_{40}$-*co*-$TgTEGMA_4$). ATRP was used to synthesize the block copolymer (Scheme 1). To this end, poly(ethylene glycol) methyl ether (mPEG) was modified with 2-bromo-2-methylpropionyl bromide to form the PEG macroinitiator. Subsequently, 2-(diisopropylamino)ethyl methacrylate (DPA) and trimethylsilyl-protected propargyltriethylene glycol methyl ether methacrylate (TMSPgTEGMA) were copolymerized using the PEG macroinitiator, copper chloride (CuCl) as the catalyst and pentamethyldiethylenetriamine

(PMDETA) as the ligand. After purification by dialysis against tetrahydrofuran (THF), the TMS protecting group was removed by treatment with tetrabutylammonium fluoride overnight to yield PEG_{45}-*b*-P(DPA_{55}-*co*-$PgTEGMA_4$).

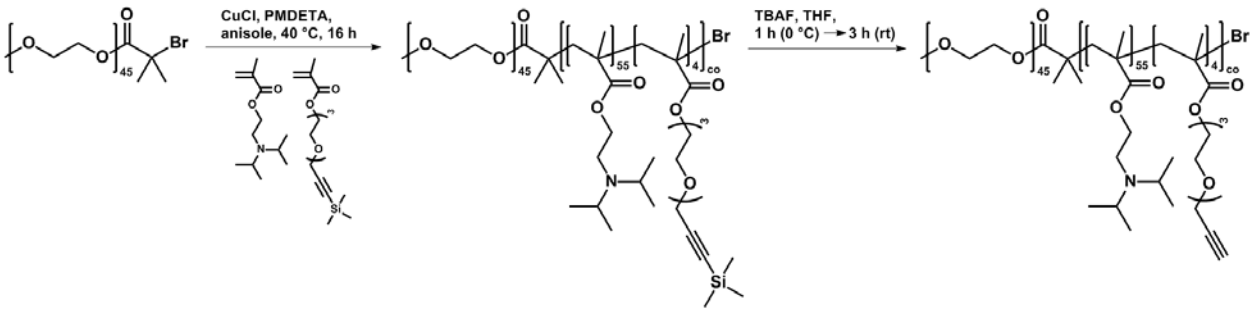

Scheme 1. Schematic representation of the synthesis of PEG_{45}-*b*-P(DPA_{55}-*co*-$PgTEGMA_4$).

The composition of the block copolymer was determined by ^1H NMR using the representative DPA (4, 6; 2.5-3.2 ppm) and TMS signal (8; 0.17 ppm) (Figure 1, top). The quantitative deprotection of the alkyne functionality was confirmed by the disappearance of the TMS signal in the spectrum of the final block copolymer (Figure 1, bottom). Size exclusion chromatography (SEC) measurements demonstrated the synthesis of a well-defined block copolymer by ATRP with M_n = 14.7 kDa and Đ < 1.3.

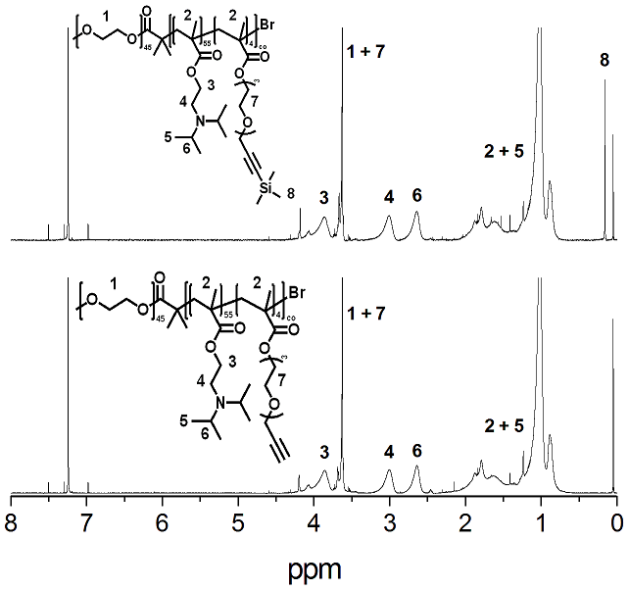

Figure 1. ^{1}H NMR spectra of (top) poly(ethylene glycol)-*block*-(2-diisopropylaminoethyl methacrylate-*co*-2-(2-(2-(prop-2-ynyloxy)ethoxy)ethoxy)ethyl methacrylate) (PEG_{45}-*b*-P(DPA_{55}-*co*-$TMSPgTEGMA_4$) synthesized by ATRP, and (bottom) the deprotected block copolymer PEG_{45}-*b*-P(DPA_{55}-*co*-$PgTEGMA_4$).

Synthesis of Polymer-Peptide Blend Replica Particles. To synthesize the polymer-peptide blend replica particles, firstly MS particles were functionalized with a layer of primary amine groups to obtain positively charged surfaces. A thin sacrificial PMA layer was then introduced at pH 4.5 (< pK_a of PMA~6.5), utilizing electrostatic forces between the positively charged MS particles and the slightly negatively charged PMA. A mixture of PHis and PEG_{45}-*b*-P(DPA_{55}-*co*-$PgTEGMA_4$), with different peptide-to-polymer ratio (1:1, 1:5, 1:10, or 1:15), was then allowed to interact with PMA at pH 4.5 (< pK_a of PHis, ~6.1[32] and of PDPA, ~6.4[26,27]). The interactions were governed by hydrogen bonding between the PEG moieties of PEG_{45}-*b*-P(DPA_{55}-*co*-$PgTEGMA_4$) and/or the imidazole ring of PHis and protonated PMA carboxyl groups as well as by electrostatic forces between the protonated tertiary amine groups of PDPA and/or the protonated imidazole ring of PHis and slightly negatively charged PMA at pH 4.5. Afterwards, the MS particle templates were removed using buffered hydrofluoric acid (HF) to obtain replica particles, without additional cross-linking. Exposure to a high pH buffer (pH 7.8) caused deprotonation of the tertiary amine groups of PDPA and imidazole rings of PHis, hence switching these moieties from hydrophilic to hydrophobic and disrupting their complementary interactions with PMA. The PMA layers were then expelled (data not shown), yielding monodisperse, bioresponsive, non-cross-linked polymer-peptide blend replica particles (Scheme 2).

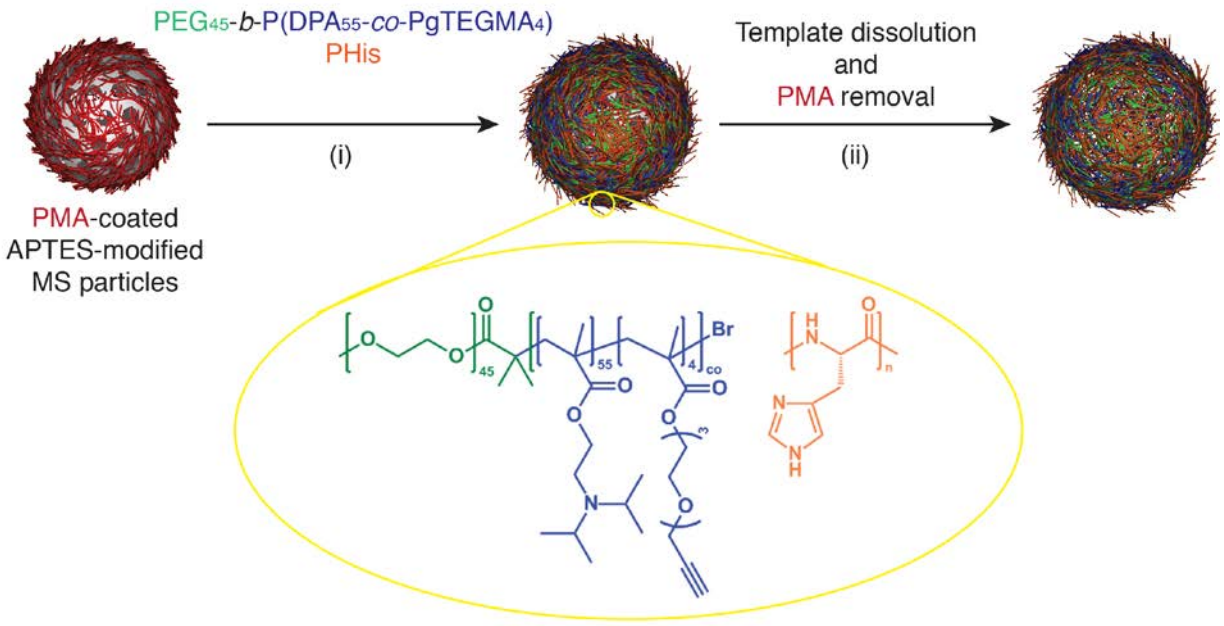

Scheme 2. Templated assembly of polymer-peptide blend replica particles. (i) The co-infiltration of PHis and PEG_{45}-*b*-P(DPA_{55}-*co*-$PgTEGMA_4$) into a 1.4 μm-diameter PMA-coated MS particle templates with different peptide-to-polymer ratios (1:1, 1:5, 1:10, or 1:15). (ii) Sacrificial template and PMA removal upon exposure to HF and high pH (pH 7.8) buffer, respectively. Monodisperse, bioresponsive, linker-free polymer-peptide blend replica particles stabilized by hydrophobic interactions are obtained.

Microscopic analysis of the particles showed the formation of spherical, disk-shaped, thick-shelled, and colloidally stable particles independent of the peptide-to-polymer ratio used (Figure 2). Smaller size particles can also be prepared using this method (Figure S2). As mentioned earlier, these particles were stable at physiological pH (PBS, pH 7.4) due to the hydrophobic interactions between PDPA and PHis, which were found to be adequate for particle stabilization for the peptide-to-polymer assembly ratios used (1:1, 1:5, 1:10, or 1:15). Single component particles made purely of PEG_{45}-*b*-P(DPA_{55}-*co*-$PgTEGMA_4$) or PHis resulted in no particles or a highly aggregated system, respectively (data not shown). The use of PDPA without

PEG copolymer, purely by itself or with a PHis blend, yielded no particle formation or a colloidally unstable and aggregated system, respectively (data not shown). Based on these findings, it is speculated that PHis provides more pronounced hydrophobic interactions compared to the PDPA moieties and other complementary forces, i.e., hydrogen bonding and π-π stacking, which serve to stabilize the particle assembly. This hypothesis was further supported by TEM analysis of the air-dried particles, which demonstrated the formation of a slightly denser particle core with a higher PHis content (Figure 2). There was no considerable swelling observed of PHis or PEG_{45}-*b*-P(DPA_{55}-*co*-$PgTEGMA_4$) at pH < pK_a (data not shown), suggesting strong hydrophobic forces caused by PHis mainly in the particle core. This was found to counteract the repulsive forces originating from protonated tertiary amine groups and imidazole rings of PDPA and PHis, respectively.

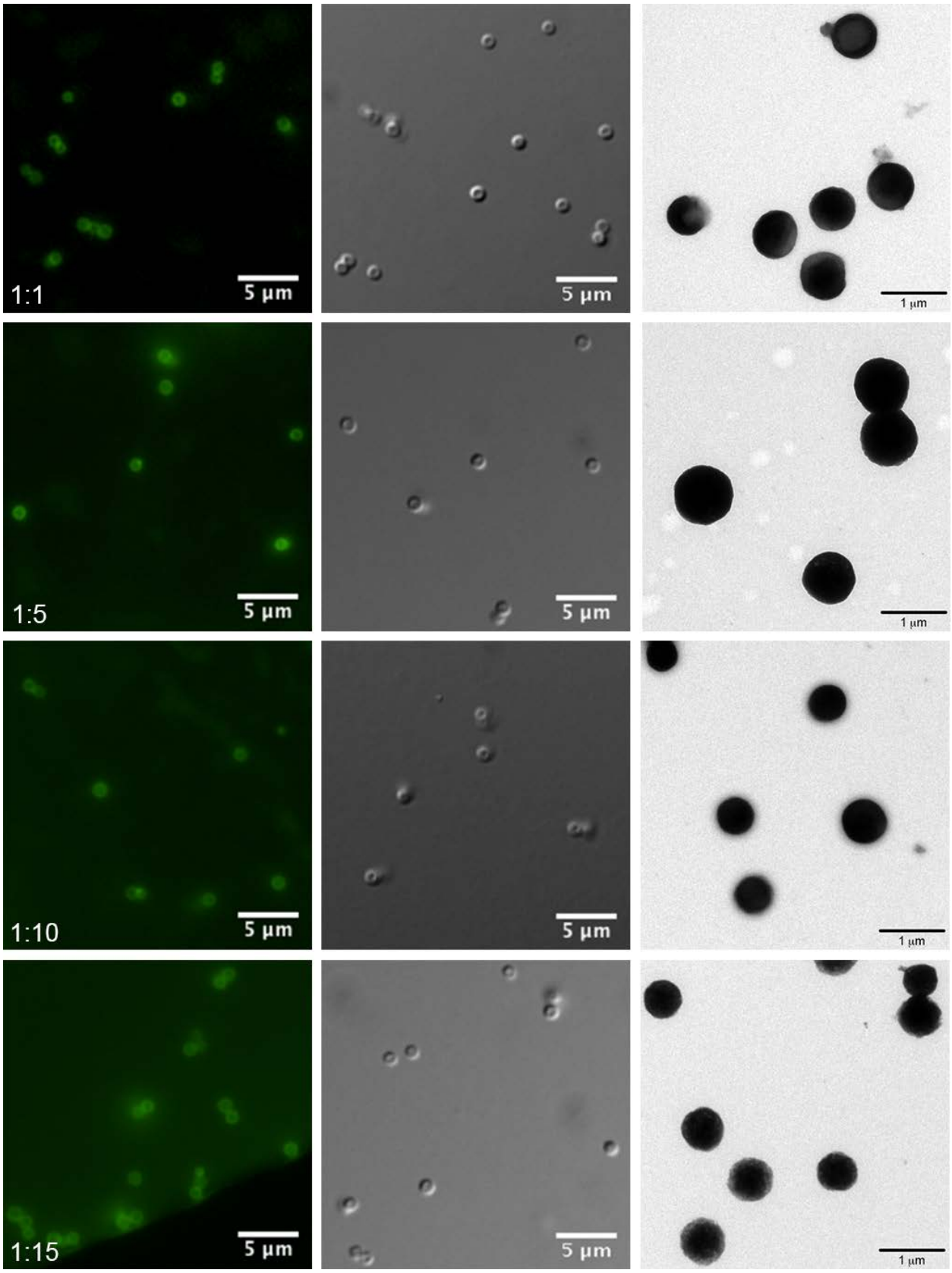
1:1
5 µm
5 µm
1 µm
1:5
5 µm
5 µm
1 µm
1:10
5 µm
5 µm
1 µm
1:15
5 µm
5 µm
1 µm

Figure 2. Microscopy images of polymer-peptide blend replica particles assembled from different peptide-to-polymer ratios (1:1, 1:5, 1:10, or 1:15). (Left column) fluorescence and (middle column) DIC microscopy images of particles dispersed in MOPS (20 mM, pH 7.8), (right column) TEM images of air-dried particles. Particles were labeled with AF488 (green). Scale bars are 5 μm for the left and middle columns, and 1 μm for the right column.

Characterization of Polymer-Peptide Blend Replica Particles. Although TEM measurements confirmed the formation of polymer-peptide blend replica particles (Figure 2), the fluorescence and DIC microscopy analysis showed a hollow-like particle core with a thick shell. Confocal laser scanning microscopy (CLSM) experiments were conducted to examine the cross-section of particles along their z-stacks. To this end, particles were fluorescently labeled with AF488 (green) using a copper(I)-catalyzed alkyne-azide cycloaddition (CuAAC) reaction. Fluorescence intensity cross-sectional profiles of the particles (Figure 3) verified the formation of polymer core networks and suggested that less material was deposited in the core, resulting in the thick shell structure observed by fluorescence and DIC microscopy.

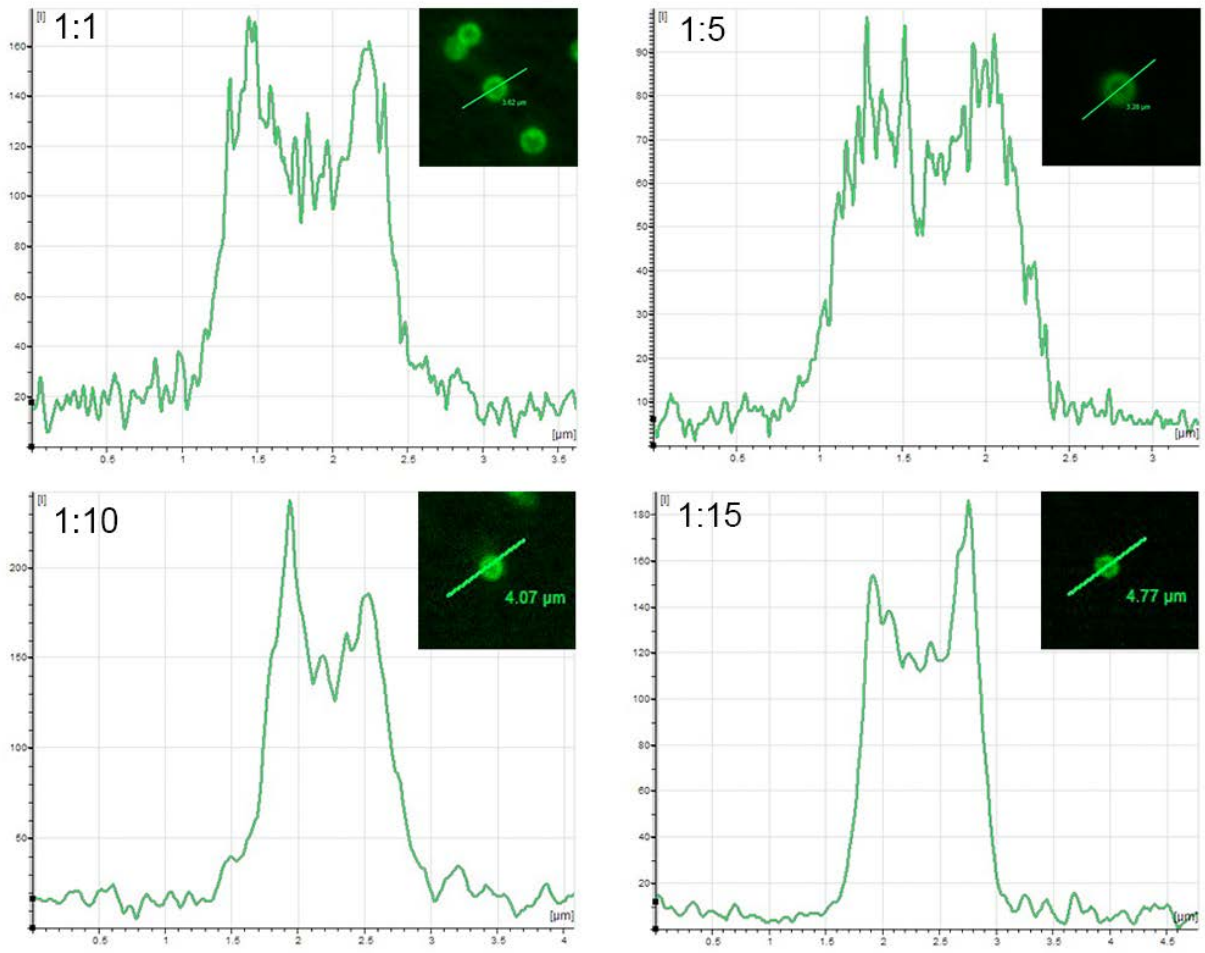

Figure 3. Fluorescence intensity profile of the polymer-peptide blend replica particles assembled from different peptide-to-polymer ratios (1:1, 1:5, 1:10, or 1:15), measured by CLSM. Particles were dispersed in MOPS (20 mM, pH 7.8) and labeled with AF488 (green).

The amount of PHis and PEG_{45}-*b*-P(DPA_{55}-*co*-$PgTEGMA_4$) infiltrated into the MS particle templates was evaluated to determine the polymer-particle blend composition for different peptide-to-polymer mixing ratios. PHis and PEG_{45}-*b*-P(DPA_{55}-*co*-$PgTEGMA_4$) were pre-labeled with AF488 dye using *N*-hydroxysuccinimide (NHS) and CuAAC chemistry, respectively. Two sets of particles, each consisting of four different peptide-to-polymer assembly ratios (1:1, 1:5, 1:10, and 1:15), were prepared using AF488-labeled PHis and non-labeled

PEG_{45}-*b*-P(DPA_{55}-*co*-$PgTEGMA_4$) or non-labeled PHis and AF488-labeled PEG_{45}-*b*-P(DPA_{55}-*co*-$PgTEGMA_4$). Following the polymer-peptide adsorption, the particles were centrifuged and the supernatant was collected for quantification. Calibration curves correlating the fluorescence intensity of AF488-labeled PHis or AF488-labeled PEG_{45}-*b*-P(DPA_{55}-*co*-$PgTEGMA_4$) were separately obtained (Figure S1) and used to evaluate the free amount of peptide or polymer in the supernatant, and hence the amount of material deposited. It was found that the actual peptide-to-polymer loading ratios are 2:1, 1:3, 1:7, and 1:21 for the 1:1, 1:5, 1:10, and 1:15 peptide-to-polymer assembly ratios, respectively (Table S1). A higher PHis content was found in the 1:1, 1:5, and 1:10 samples, suggesting more effective infiltration of PHis compared to PEG_{45}-*b*-P(DPA_{55}-*co*-$PgTEGMA_4$) albeit their similar pK_a values. The smaller imidazole ring structure of PHis, compared to the PEG_{45}-*b*-P(DPA_{55}-*co*-$PgTEGMA_4$) side chain could be the driving force for material adsorption to the confined space within the MS particle templates. However, the opposite was observed when the peptide-to-polymer ratio was significantly lower, as found in the 1:15 particles.

Stability and Degradation of Polymer-Peptide Blend Replica Particles. As the synthesized particles are non-cross-linked, the stability of these particles is mainly governed by the non-covalent hydrophobic interactions between the PHis and PEG_{45}-*b*-P(DPA_{55}-*co*-$PgTEGMA_4$) at physiological pH (pH 7.4). To test their stability, the particles were incubated at simulated physiological conditions (PBS pH 7.4, 37 °C). Flow cytometry was used to count the particles over a time range of 24 h (Figure S3). All particles were found to be considerably stable over the course of the experiments, demonstrating that hydrophobic interactions were sufficient for stabilizing the particles.

The degradability of these polymer-peptide blend replica particles was then investigated. A typical pathway for the cellular internalization of particulate carriers follows an endocytosis mechanism, in which the carriers are dynamically transported from endosomes (pH 6.8–5.9) to lysosomes (pH 6.0–4.9).[22,23] Various proteases are present in these cellular compartments. Therefore, particle degradability at an endolysosomal microenvironment becomes an interesting carrier property. As the particles are a blend of a polymer and a peptide with similar pK_a values (~6.1 for PHis and ~6.4 for PDPA), degradation of these particles can be triggered by a pH decrease from physiological (pH 7.4) to endolysosomal (pH 4.9–6.8) pH and by the presence of protease. Different compositions of the polymer-particle blends were expected to provide control over particle degradation kinetics. Thus, to investigate their degradability, particles were exposed to simulated endosomal conditions *in vitro* (PBS pH 5.5, 37 °C, 5 unit mL^{-1} protease) and the particle count was then monitored using flow cytometry for up to 6 h.

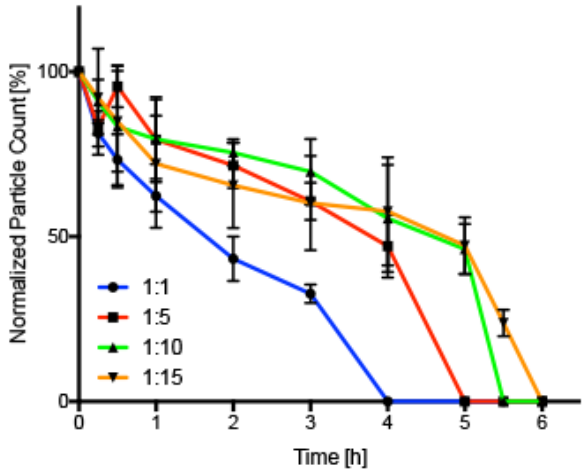

Figure 4. Degradation profile of the polymer-peptide blend replica particles, based on protease-induced hydrolysis for different peptide-to-polymer assembly ratios; 1:1 (blue circles), 1:5 (red squares), 1:10 (green triangles), 1:15 (orange inverted triangles). Particles were exposed to simulated endosomal conditions (5 units mL^{-1} protease, PBS pH 5.5, and 37 °C) with constant

shaking (800 rpm). The particle count was followed by flow cytometry. Experiments were performed in triplicate.

The degradation profiles showed tunable degradation kinetics for the particles, based on the peptide/polymer content within the particles, ranging from 4 h to 6 h (Figure 4). Particles with the highest peptide content (1:1 peptide-to-polymer assembly ratio) showed the fastest degradation rate (4 h). The degradation rate was found to be slower with a decrease in the peptide proportion, which supports the finding that PHis is the main component of the particle core with PEG_{45}-*b*-P(DPA_{55}-*co*-$PgTEGMA_4$) in the periphery. The pH decrease, which causes protonation of PDPA and PHis, was found to play a minor role in governing the degradation. As noted above, the strong hydrophobic forces of PHis may compensate the repulsive forces between the protonated groups of PDPA and PHis. Hence, protease becomes the essential trigger for particulate degradation.

Intracellular Properties of Polymer-Peptide Blend Replica Particles. Interactions of particulate carriers with cellular microenvironments are important in designing bioresponsive materials for biomedical applications. JAWS II cells are immortalized dendritic cell lines extracted from primary mouse bone marrow.[47] DCs are useful in regulating the immune system due to their role as antigen presenting cells.[48-50] Particle cytotoxicity was first examined by incubating particles, assembled using different peptide-to-polymer ratios (1:1, 1:5, 1:10, or 1:15), with JAWS II cells for 48 h. XTT assays showed negligible cytotoxicity, even at a high particle-to-cell ratio (100:1) for all polymer-peptide blends (Figure S4). The cell association/internalization kinetics was then examined to evaluate particle uptake by JAWS II cells. Particles were labeled with AF488 (green) and incubated at a 20:1 particle-to-cell ratio for

6 h with hourly sampling (Figure S5). The kinetics were evaluated by monitoring the fluorescence intensity of the particles inside the cells using flow cytometry. These experiments demonstrated particle association/internalization over 6 h. A similar behavior was observed for all polymer-peptide blends at 1 h. Therefore, an incubation time of 1 h was used to ensure equivalent intracellular interactions among all polymer-peptide blends, hence enabling comparative analysis of the particle intracellular degradation kinetics *in vitro* inside JAWS II cells.

Intracellular degradation kinetics were monitored using a fluorophore-quencher pair. Particles were prepared from AF488-labeled PHis and BHQ1-labeled PEG_{45}-*b*-P(DPA_{55}-*co*-$PgTEGMA_4$). Negligible and complete degradation are indicated by virtually no fluorescence and bright green fluorescence, respectively. The particles were added at a 20:1 particle-to-cell ratio to JAWS II cells for 1 h. The cell media was aspirated and replaced with warm cell media (37 °C) to remove unbound particles and ensure a reliable comparison of particle degradation kinetics. The cells were imaged live using a deconvolution microscope using an *in situ* setup cellular microenvironment (37 °C, 5% CO_2) at different times (2, 4, 6, 8, 10, and 18 h).

Bright green fluorescence fragmentation throughout the cells indicated particle degradation *in vitro* inside the cells. Live cell imaging demonstrated that degradation was achieved after 2, 4, 6, and 8 h for polymer-peptide blend replica particles assembled from 1:1, 1:5, 1:10, 1:15 peptide-to-polymer ratios, respectively (Figure 5), suggesting the tunable biodegradation of these particles. At the shorter incubation times, a small number of green fluorescence dots without any fragmentations were observed (less than 5% of the total cell population). We speculate that the pH decrease inside endo/lysosomes caused protonation of the tertiary amine groups of PDPA and the imidazole rings of PHis, which might lead to charge

repulsion inside the core and thus, to an incomplete quenching of the components. However, the degradation of the particles, as indicated by the bright fluorescence fragmentation, is in accordance with the degradation kinetics observed under simulated endosomal conditions. A higher PHis content led to faster degradation of the carriers, probably because of the presence of a large variety of proteases inside the cells that accelerate the hydrolysis of PHis. Longer incubation time (10 h and 18 h) resulted in the complete degradation of particles with no significant peptide/polymer blends visible (Figures S6 and S7).

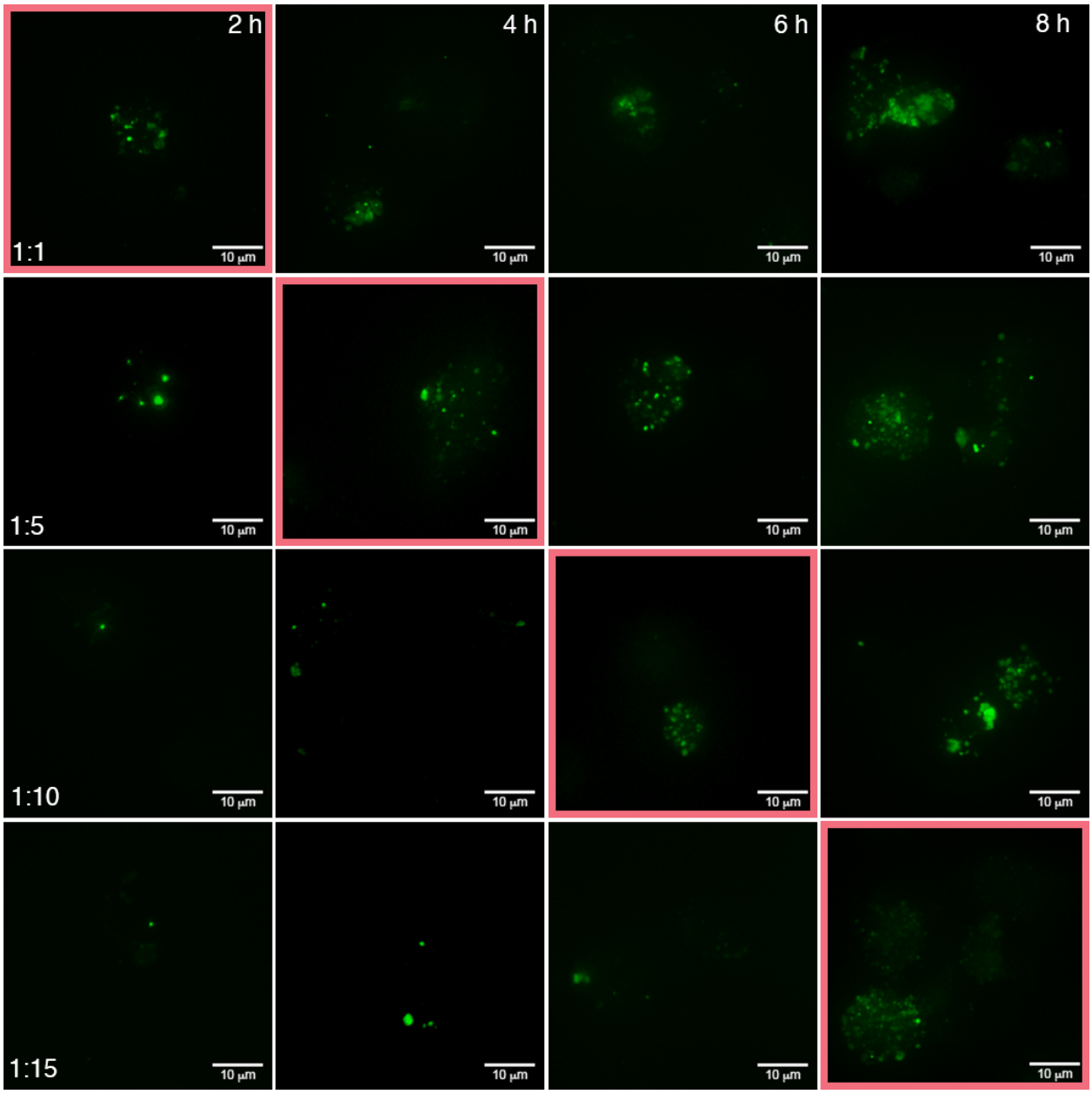

Figure 5. Representative deconvolution optical microscopy images (with maximum intensity projection) of the intracellular degradation of polymer-peptide blend replica particles, assembled from different peptide-to-polymer ratios (1:1, 1:5, 1:10, or 1:15), in JAWS II cells for 2, 4, 6, and 8 h. PHis was labeled with AF488 (green) and PEG_{45}-*b*-P(DPA_{55}-*co*-$PgTEGMA_4$) was labeled with BHQ1 to quench the fluorescence from PHis. The red-bordered images indicate the time at

which the particles were found to be degraded (>40% of the total cell population). Scale bars are 10 μm.

CONCLUSIONS

We have demonstrated the MS templated assembly of polymer-peptide blends replica particles via co-infiltration of PHis and PEG_{45}-*b*-P(DPA_{55}-*co*-$PgTEGMA_4$) assembled from different polymer-to-peptide ratios (1:1, 1:5, 1:10, or 1:15) without additional cross-linking. The similarity in the pK_a values of PDPA (~6.4) and PHis (~6.1) allows a switch in property of the particles from hydrophilic to hydrophobic, which was utilized for carrier stabilization. Microscopy and flow cytometry experiments demonstrated the formation of stable replica particles. *In vitro* degradation experiments at endosomal conditions (pH 5.5, protease 5 units mL^{-1}) imparted tunable kinetics upon varying the peptide-to-polymer content. This was further verified by an *in vitro* intracellular degradation experiment in a vaccine model cell line, JAWS II. The analysis confirmed that particle biodegradability could be engineered from 2 to 8 h for different peptide-to-polymer ratios used. The use of innate material properties to induce carrier assembly and disassembly, and to tailor the degradation kinetics is an interesting and a highly modular approach to design particles that are responsive to certain environmental stimuli.

ASSOCIATED CONTENT

Supporting Information. TEM images of smaller polymer-peptide blend replica particles (200 and 700 nm), calibration curves for AF488-labeled PHis and AF488-labeled PEG_{45}-*b*-P(DPA_{55}-*co*-$PgTEGMA_4$), quantification of the amount of PHis and PEG_{45}-*b*-P(DPA_{55}-*co*-$PgTEGMA_4$)

adsorbed into the MS particles, stability of the polymer-peptide blend replica particles, XTT assays, particle-to-cell association kinetics, and deconvolution microscopy images of the intracellular degradation are provided in the Supporting Information. This material is available free of charge via the Internet at http://pubs.acs.org.

AUTHOR INFORMATION

Corresponding Author

*E-mail: fcaruso@unimelb.edu.au.

Present Addresses

[+]Department of Chemistry, University of Warwick, CV 4 7AL, Coventry, UK

[‡]Department of Chemistry, The University of Melbourne, Parkville, Victoria 3010, Australia

[#]CSIRO Process Science and Engineering, Clayton, Victoria 3168, Australia

[§]Drug Delivery, Disposition and Dynamics, Monash Institute of Pharmaceutical Sciences, Monash University, Parkville, Victoria 3052, Australia

ACKNOWLEDGMENTS

This research was funded by the Australian Research Council Centre of Excellence in Convergent Bio-Nano Science and Technology (CE140100036) and by the Australian Research Council under the Australian Laureate Fellowship (F.C., FL120100030), Super Science Fellowship (F.C., FS110200025), and Australian Future Fellowship (G.K.S., FT120100564, and A.P.R.J., FT110100265) schemes. K. Kempe is grateful to the Alexander von Humboldt-Foundation for a Feodor-Lynen Fellowship.

REFERENCES

1. Langer, R. S., *Nature* **1998,** *392*, 5-10.
2. Haag, R.; Kratz, F., *Angew. Chem. Int. Ed.* **2006,** *45*, 1198-1215.
3. Discher, D. E.; Eisenberg, A., *Science* **2002,** *297*, 967-973.
4. Ariga, K.; Lvov, Y. M.; Kawakami, K.; Ji, Q.; Hill, J. P., *Adv. Drug Delivery Rev.* **2011,** *63*, 762-771.
5. Ge, Z.; Liu, S., *Chem. Soc. Rev.* **2013,** *42*, 7289-7325.
6. Kataoka, K.; Harada, A.; Nagasaki, Y., *Adv. Drug Delivery Rev.* **2001,** *47*, 113-131.
7. Discher, D. E.; Ahmed, F., *Annu. Rev. Biomed. Eng.* **2006,** *8*, 323-341.
8. Johnston, A. P. R.; Cortez, C.; Angelatos, A. S.; Caruso, F., *Curr. Opin. Colloid Interface Sci.* **2006,** *11*, 203-209.
9. Cui, J.; van Koeverden, M. P.; Mullner, M.; Kempe, K.; Caruso, F., *Adv. Colloid Interface Sci.* **2014,** *207C*, 14-31.
10. Wang, Y.; Price, A. D.; Caruso, F., *J. Mater. Chem.* **2009,** *19*, 6451-6464.
11. Uhrich, K. E.; Cannizzaro, S. M.; Langer, R. S.; Shakesheff, K. M., *Chem. Rev.* **1999,** *99*, 3181-3198.
12. Duncan, R., *Curr. Opin. Biotechnol.* **2011,** *22*, 492-501.
13. Theato, P.; Sumerlin, B. S.; O'Reilly, R. K.; Epps, I. I. I. T. H., *Chem. Soc. Rev.* **2013,** *42*, 7055-7056.
14. Stuart, M. A. C.; Huck, W. T. S.; Genzer, J.; Müller, M.; Ober, C.; Stamm, M.; Sukhorukov, G. B.; Szleifer, I.; Tsukruk, V. V.; Urban, M.; Winnik, F.; Zauscher, S.; Luzinov, I.; Minko, S., *Nat. Mater.* **2010,** *9*, 101-113.
15. Russell, T. P., *Science* **2002,** *297*, 964-967.

16. De Geest, B. G.; Sanders, N. N.; Sukhorukov, G. B.; Demeester, J.; De Smedt, S. C., *Chem. Soc. Rev.* **2007,** *36*, 636-649.

17. Carregal-Romero, S.; Ochs, M.; Rivera-Gil, P.; Ganas, C.; Pavlov, A. M.; Sukhorukov, G. B.; Parak, W. J., *J. Controlled Release* **2012,** *159*, 120-127.

18. Chen, W.; Du, J., *Sci. Rep.* **2013,** *3*, DOI: 10.1038/srep02162.

19. de la Rica, R.; Aili, D.; Stevens, M. M., *Adv. Drug Delivery Rev.* **2012,** *64*, 967-978.

20. Fleige, E.; Quadir, M. A.; Haag, R., *Adv. Drug Delivery Rev.* **2012,** *64*, 866-884.

21. Canton, I.; Battaglia, G., *Chem. Soc. Rev.* **2012,** *41*, 2718-2739.

22. Huotari, J.; Helenius, A., *EMBO J.* **2011,** *30*, 3481-3500.

23. Maxfield, F. R.; Yamashiro, D. J., *Adv. Exp. Med. Biol.* **1987,** *225*, 189-198.

24. Casey, J. R.; Grinstein, S.; Orlowski, J., *Nat. Rev. Mol. Cell Biol.* **2010,** *11*, 50-61.

25. Pillay, C. S.; Elliott, E.; Dennison, C., *Biochem. J.* **2002,** *363*, 417-429.

26. Lomas, H.; Canton, I.; MacNeil, S.; Du, J.; Armes, S. P.; Ryan, A. J.; Lewis, A. L.; Battaglia, G., *Adv. Mater.* **2007,** *19*, 4238-4243.

27. Lomas, H.; Massignani, M.; Abdullah, K. A.; Canton, I.; Lo Presti, C.; MacNeil, S.; Du, J.; Blanazs, A.; Madsen, J.; Armes, S. P.; Lewis, A. L.; Battaglia, G., *Faraday Discuss.* **2008,** *139*, 143-159.

28. Yu, H.; Zou, Y.; Wang, Y.; Huang, X.; Huang, G.; Sumer, B. D.; Boothman, D. A.; Gao, J., *ACS Nano* **2011,** *5*, 9246-9255.

29. Zhou, K.; Liu, H.; Zhang, S.; Huang, X.; Wang, Y.; Huang, G.; Sumer, B. D.; Gao, J., *J. Am. Chem. Soc.* **2012,** *134*, 7803-7811.

30. Du, J.; Tang, Y.; Lewis, A. L.; Armes, S. P., *J. Am. Chem. Soc.* **2005,** *127*, 17982-17983.

31. Du, J.; Fan, L.; Liu, Q., *Macromolecules* **2012,** *45*, 8275-8283.

32. Yang, S. R.; Lee, H. J.; Kim, J.-D., *J. Controlled Release* **2006,** *114*, 60-68.

33. De Geest, B. G.; Vandenbroucke, R. E.; Guenther, A. M.; Sukhorukov, G. B.; Hennink, W. E.; Sanders, N. N.; Demeester, J.; De Smedt, S. C., *Adv. Mater.* **2006,** *18*, 1005-1009.

34. Tansey, W.; Ke, S.; Cao, X. Y.; Pasuelo, M. J.; Wallace, S.; Li, C., *J. Controlled Release* **2004,** *94*, 39-51.

35. Cui, J. W.; Yan, Y.; Wang, Y. J.; Caruso, F., *Adv. Funct. Mater.* **2012,** *22*, 4718-4723.

36. Mertz, D.; Tan, P.; Wang, Y.; Goh, T. K.; Blencowe, A.; Caruso, F., *Adv. Mater.* **2011,** *23*, 5668-5673.

37. Mullner, M.; Cui, J.; Noi, K. F.; Gunawan, S. T.; Caruso, F., *Langmuir* **2014,** *30*, 6286-6293.

38. Wang, Y.; Caruso, F., *Adv. Mater.* **2006,** *18*, 795-800.

39. Liang, K.; Richardson, J. J.; Ejima, H.; Such, G. K.; Cui, J.; Caruso, F., *Adv. Mater.* **2014,** *26*, 2398-2402.

40. Liang, K.; Such, G. K.; Johnston, A. P. R.; Zhu, Z.; Ejima, H.; Richardson, J. J.; Cui, J.; Caruso, F., *Adv. Mater.* **2014,** *26*, 1901-1905.

41. Liang, K.; Gunawan, S. T.; Richardson, J. J.; Such, G. K.; Cui, J.; Caruso, F., *Adv. Healthcare Mater.* **2014,** *3*, 1551-1554.

42. Liang, K.; Such, G. K.; Zhu, Z.; Dodds, S. J.; Johnston, A. P. R.; Cui, J.; Ejima, H.; Caruso, F., *ACS Nano* **2012,** *6*, 10186-10194.

43. Liang, K.; Such, G. K.; Zhu, Z.; Yan, Y.; Lomas, H.; Caruso, F., *Adv. Mater.* **2011,** *23*, H273-H277.

44. Gunawan, S. T.; Liang, K.; Such, G. K.; Johnston, A. P.; Leung, M. K.; Cui, J.; Caruso, F., *Small* **2014,** DOI: 10.1002/smll.201400450.

45. Wei, H.; Ravarian, R.; Dehn, S.; Perrier, S.; Dehghani, F., *J. Polym. Sci., Part A: Polym. Chem.* **2011,** *49*, 1809-1820.

46. Wang, J.-G.; Zhou, H.-J.; Sun, P.-C.; Ding, D.-T.; Chen, T.-H., *Chem. Mater.* **2010,** *22*, 3829-3831.

47. Jiang, X.; Shen, C.; Rey-Ladino, J.; Yu, H.; Brunham, R. C., *Infect. Immun.* **2008,** *76*, 2392-2401.

48. Shortman, K.; Liu, Y. J., *Nat. Rev. Immunol.* **2002,** *2*, 151-161.

49. Steinman, R. M., *Annu. Rev. Immunol.* **1991,** *9*, 271-296.

50. Steinman, R. M.; Nussenzweig, M. C., *Proc. Natl. Acad. Sci. U.S.A.* **2002,** *99*, 351-358.

TOC

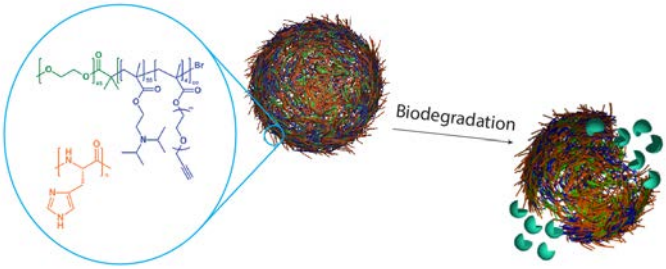

Author/s:
Gunawan, ST; Kempe, K; Such, GK; Cui, J; Liang, K; Richardson, JJ; Johnston, APR; Caruso, F

Title:
Tuning Particle Biodegradation through Polymer-Peptide Blend Composition

Date:
2014-12-01

Citation:
Gunawan, S. T., Kempe, K., Such, G. K., Cui, J., Liang, K., Richardson, J. J., Johnston, A. P. R. & Caruso, F. (2014). Tuning Particle Biodegradation through Polymer-Peptide Blend Composition. BIOMACROMOLECULES, 15 (12), pp.4429-4438. https://doi.org/10.1021/bm5012272.